

Article

Study on Anchorage Performance of New High-Strength Fast Anchorage Agent

Haifeng Li ^{1,*}, Kun Wang ^{1,*} , Zizhang Dong ¹ and Tao Liu ^{2,3}¹ College of Environmental Science and Engineering, Ocean University of China, Qingdao 266100, China² Shandong Provincial Key Laboratory of Marine Environment and Geological Engineering, Ocean University of China, Qingdao 266100, China³ Pilot National Laboratory for Marine Science and Technology, Qingdao 266061, China

* Correspondence: cohenwang@foxmail.com

Abstract: To achieve the efficient, rapid construction of prestressed anchor cables, in this study, through an indoor pull-out test and field basic test, we investigated the mechanical behavior, expansion, drawing performance and bond properties of a new type of high-strength, fast anchorage agent. We analyzed the influence of the water material ratio and curing time on its performance and determined the corresponding construction. It was found that the new anchoring agent could be effectively applied in field construction and achieved a compressive strength of 30 MPa within 30 h. Moreover, during the solidification process, the hydration reaction node could be reached within 5–6 h when the material expansion was and the feedback to the water–material ratio were the strongest. In addition, in the drawing process, the anchorage agent exhibited a strong bond with the reinforcement and the rock layer, and the bonding of the anchorage agent to the rock layer was greater than that of the steel bar. Therefore, in order to provide anchorage, it is necessary to increase the contact area between the steel strand and the anchorage agent.

Keywords: new anchorage agent; test of anchorage performance; water–material ratio; curing time; mechanical behavior



Citation: Li, H.; Wang, K.; Dong, Z.; Liu, T. Study on Anchorage Performance of New High-Strength Fast Anchorage Agent. *Appl. Sci.* **2022**, *12*, 8494. <https://doi.org/10.3390/app12178494>

Academic Editor: Daniel Dias

Received: 8 July 2022

Accepted: 23 August 2022

Published: 25 August 2022

Publisher's Note: MDPI stays neutral with regard to jurisdictional claims in published maps and institutional affiliations.



Copyright: © 2022 by the authors. Licensee MDPI, Basel, Switzerland. This article is an open access article distributed under the terms and conditions of the Creative Commons Attribution (CC BY) license (<https://creativecommons.org/licenses/by/4.0/>).

1. Introduction

Prestressed anchoring technology is widely used for slopes, deep foundation pits and other types of geotechnical engineering. This technology's geotechnical physical capacity, geotechnical strength and self-supporting capacity can be fully utilized to ensure construction safety.

The basic domestic anchorage engineering of bonding materials uses ordinary cement mortar, but the slow hardening and early strength growth during cement hydration condensation are time-consuming, and that it usually takes such cement 14–28 days to solidify to a degree that meets tensioning requirements. This can easily affect the project construction schedule to a certain extent and lead to economic losses. For example, if the tension is not qualified, the process needs to be started all over again, and this will certainly result in the time of projects being extended. Therefore, how to speed up the construction of prestressed anchor cables has aroused widespread interest in the engineering field.

In this context, some scholars have tried using fast-anchoring materials. For example, resin anchoring agent has the characteristics of being fast-setting and having a rapid hardening speed, fast strength growth and high strength, allowing to be applied in mine production [1–3]. Coil-type high and early strength anchoring agents have a slight expansion effect. They can achieve quick setting, early strength, water reduction, expansion and high strength when they meet water [4], and they are especially used for bolt support, foundation reinforcement, prestressed tension bolts and anchor cables in various underground engineering and emergency engineering contexts [5,6]. Although resin anchoring agents and drug-coil high-early-strength anchoring agents have the characteristics of fast setting

and early strength, the high unit prices of these materials seriously affect the popularization and application of fast-anchoring technology. Therefore, based on the requirements of fast-anchorage construction, we conducted a compressive strength test, an in-hole solidification strain test and a free solidification strain test on a new, high-strength, fast anchorage agent so as to determine its basic performance.

At present, cement mortar is primarily used as the basic bonding material for the anchoring section of prestressed anchor cables in China. However, cement mortar has a long setting time of and slow development of early strength. In anchor cable engineering, it is generally necessary to stretch the cable after 7 days, and the prestress cannot be applied to the rock mass in a short period of time. In addition, if the anchor cable does not meet qualifications, the construction period is increased due to the need for re-filling of the anchor and tensioning. Due to the poor tensile performance of cement mortar [7,8], it is easy to produce cracks in the grouting body under tensile load, which leads to corrosion of steel strands and the durability of prestressed anchor cables is greatly affected [9–11].

In order to remedy the defects of cement mortar mentioned above, a new, high-strength, fast anchorage agent should meet the following basic requirements: water resistance, acid and alkali resistance, salt resistance, fatigue resistance and aging resistance. It should be able to be cured quickly at room temperature, the early strength should develop quickly and the construction period should be shortened. On the basis of meeting the requirement for fast tensioning, it should have high tensile strength. It should have good adhesion to rock mass and metal.

2. The Hydration Principle of the High-Strength, Fast Anchorage Agent

Based on the requirements for the rapid construction of an anchor cable for Qingdao metro, a new, high-strength, fast anchorage agent that could meet the requirements of the subway construction period was developed. This material achieved the desired effect through a mixture of material A and material B, as shown in Figure 1. It had basic characteristics such as controllable setting time, high early strength, micro-expansion, frost resistance, impermeability, low alkalinity and corrosion resistance.

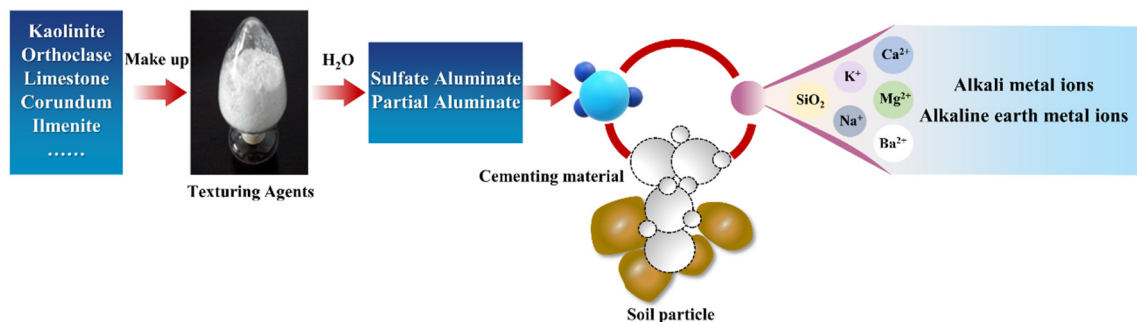


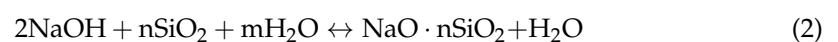
Figure 1. Reaction principle of new, high-strength, fast anchor.

The active SiO_2 content in the new, high-strength, fast anchorage agent was relatively high and could react with $\text{Ca}(\text{OH})_2$ to produce calcium silicate hydrate ($2\text{CaO} \cdot \text{SiO}_2 \cdot n\text{H}_2\text{O}$). The equation is as follows:

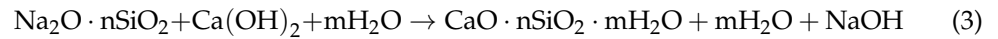


Hydrated calcium silicate is an amorphous crystalline hydride with high plastic strength and large expansion ability.

The new, high-strength, fast anchoring agent reacts with water to generate NaOH , and NaOH reacts with active SiO_2 to generate a large amount of sodium silicate. The equation is as follows:



The sodium silicate generated in the above formula reacts with $\text{Ca}(\text{OH})_2$ in the solution to produce an amorphous gel with high plastic strength—calcium silicate hydrate. The equation is as follows:



The use of calcium silicate hydrate to fill in the pores, cracks and holes of a formation or as cement is beneficial for the improvement of the strength and stability of the anchor solid.

3. Series Tests of Anchorage Performance of New Anchorage Agent

3.1. Compressive Strength of Material

After the previous material test, it was found that the effective water-to-material ratio of the new anchoring agent was about 0.25 ± 0.5 . Beyond this range, the slurry was too viscous or had insufficient strength, so this test only considered the rule of change for the compressive strength of the new anchoring agent within the effective water-to-material ratio range, along with the rule of change for the water-to-material ratio and the curing time.

The compressive strength test and research for the new type of anchorage utilized side lengths of $70.7 \times 70.7 \times 70.7$ mm to obtain sanlian mortar test standard specimens made in 70.7 mm cubes, with water material ratios of 0.22, 0.25 and 0.28. Three sets of samples were, and each sample included nine cubes. Each set of three samples had the same curing times of 1 d, 2 d and 3 d, respectively. The arithmetic mean of the three samples was used as the compressive strength value. The specific test scheme is shown in Figure 2.

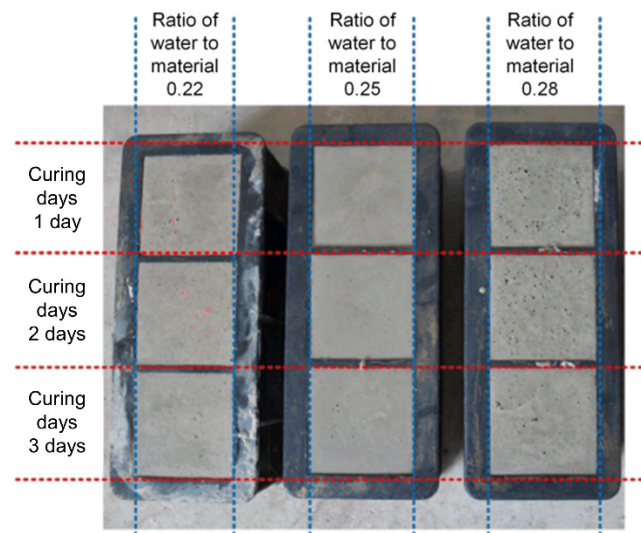


Figure 2. Test scheme for compressive strength.

3.2. Free Solidification Strain Test Scheme

In order to analyze the strain on the new, high-strength, fast anchorage agent in the process of setting and hardening, a free solidification strain test was carried out in a flexible plastic mold, as shown in Figure 3. Before the test, strain gauges were pasted onto the side and bottom of the customized, flexible plastic mold. During the solidification and hardening process, the slurry exerts pressure on the inner wall of the mold, which makes it slightly deformed. This deformation can be measured by strain gauges. The strain gauges used were BX120-3AA strain gauges with a sensitive grille size of 3×2 mm, and the nominal resistance value was 120Ω . Accordingly, the free solidification strain of the anchorage agent could be monitored in real time through a DH3816N acquisition instrument. For the DH3816N, the strain test was conducted with a 1/4 bridge, and the instrument was programmed and set by the software and connected to a PC via WIFI.

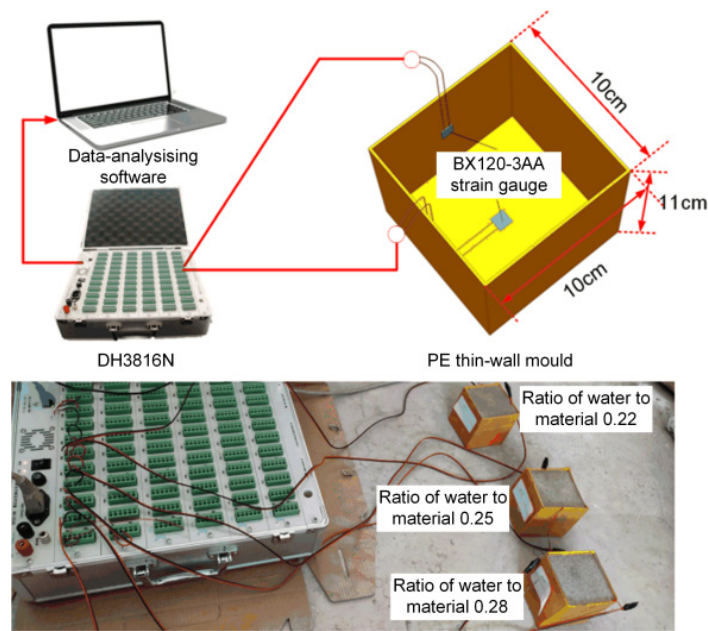


Figure 3. Free solidification strain test scheme.

3.3. Test Scheme for Solidification Strain in Hole

In order to simulate the local engineering geological conditions in Qingdao, coarse granites were used. In order to simulate the condensation strain and the filling of the new, high-strength, fast anchorage agent in the rock mass, drilling, reinforcing bars and grouting were used in the test block of the coarse granites.

As shown in Figure 4, the length, width and height of the granite test block were 10 cm, 10 cm and 20 cm, respectively. The drill hole was drilled along the height direction into the test block with a diameter of 3 cm and a depth of 15 cm. Strain gauges were affixed 15 mm from the hole bottom (C2), 15 mm from the hole mouth (C1) and 35 mm from the steel bar end (J). The strain gauges were bonded and fixed by applying epoxy AB adhesive. After curing with epoxy resin, the strain gauges had high insulation, compression resistance and bonding strength. During the test, the grouting water scores were 0.22, 0.25 and 0.28. Before grouting, HRB335 hot-rolled ribbed steel bars with a diameter of 10 mm were inserted into the center of the hole, and in-hole grouting was carried out under the condition that the reinforcement was upright. After grouting, the test block was cured for 3 days under standard conditions. Strain data were collected in real time with a DH3816N acquisition instrument so as to analyze the influence of the new, high-strength, fast anchorage agent on the rock wall and reinforcement when it solidified and hardened in the coarse-grained granite.

3.4. Pull-Out Test

In order to simulate the local engineering geological conditions in Qingdao, a hole was drilled into the coarse granite test block (diameter: 30 mm, depth: 70 mm), the test block was reinforced (a HRB335 hot-rolled ribbed steel bar with diameter of 10 mm was inserted vertically into the middle) and subjected to grouting and the pull-out test was carried out after grouting for 24 h following maintenance. The samples were divided into four groups according to the different grouting water-to-feed ratios, which were 0.22, 0.25, 0.28 and 0.31, respectively. Meanwhile, strain gauges were arranged on the hole wall, under the hole, at the bottom of the hole and in the middle of the reinforcement to measure the micro-strain in the drawing process of the granite samples so as to evaluate the bonding performance of the new anchorage agent. The test process is shown in Figure 5.

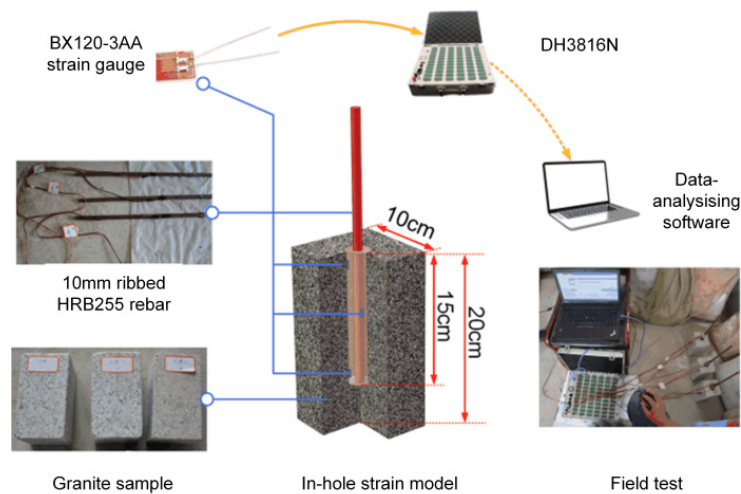


Figure 4. In-hole strain test set-up.

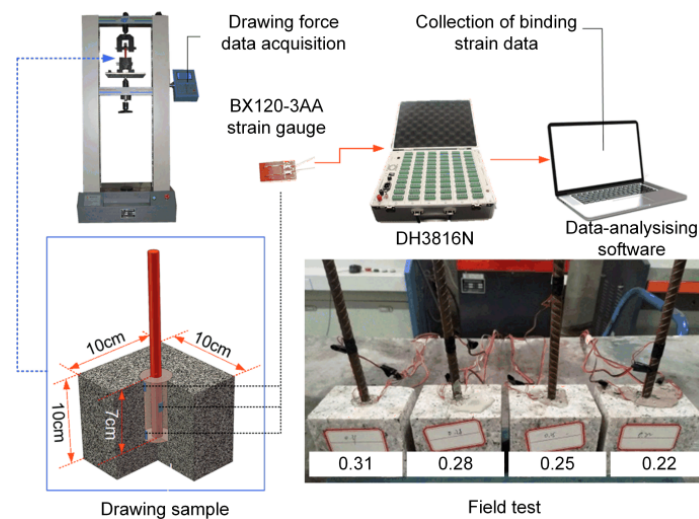


Figure 5. Pull-out test specimen.

3.5. Field Basic Test

In order to further verify the anchoring performance of the new type of anchoring agent, the construction site of the shield shaft starting from the foundation pit of the Chuang-Shi interval of Qingdao Metro Line 6 was selected as the site for the basic anchor grouting test based on the new type of high-strength, fast anchoring agent.

3.5.1. Overview of the Test Site

The shield shaft in the interval between Chuangzhigu Station and Shishan Road Station is the first phase of Qingdao Metro Line 6. The enclosure structure of the shield shaft is as follows: the upper foundation pit adopts the supporting form of “steel pipe pile + anchor cable”, and the clearance size in the section is 31.2 m (the direction along the road) × 25.4 m. The supporting form of “steel pipe pile + rock bolt” is adopted for the lower foundation pit. In order to meet the initial needs of shield tunneling, a temporary secondary lining is installed on the inner side wall and floor of the well. With the temporary secondary lining, the clearance size in the section is 28 m (the direction along the road) × 22.4 m. The initial well depth is 34.0 m. The formation in which the starting well is located is distributed from top to bottom in the order of plain filling, strong ~ medium ~ breezed granite and granite porphyry, and there are joint and fracture zones locally.

3.5.2. Test Anchor Cable Setting

To ensure the validity of the test, two test anchor cables were set at the profile location in representative rock and soil. They were located in the north side of the foundation pit, as shown in Figures 6 and 7. The first-layer anchor cables MS1'-N1 (northwest corner of the foundation pit) and MS1'-N21 (northeast corner of the foundation pit) were selected. Anchor cable parameters were set according to the design shown in Table 1.

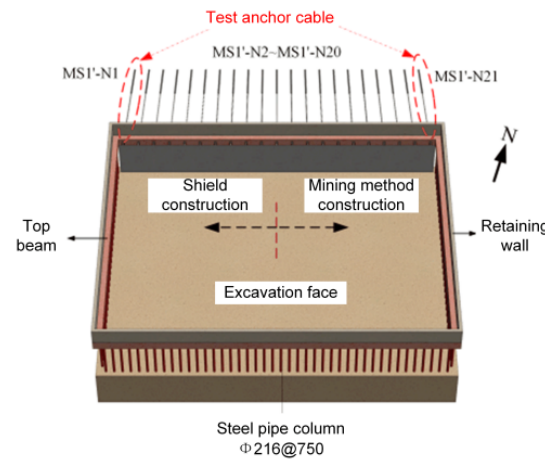


Figure 6. Construction position of test anchor cable.

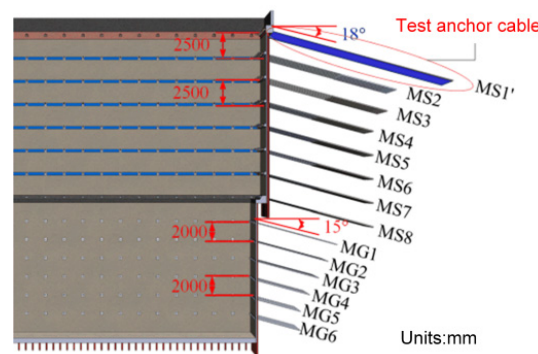


Figure 7. Anchorage construction section.

Table 1. Test anchor cable parameters.

| Anchor Number | MS1'-N1 | MS1'-N21 |
|---|---------|----------|
| Specification for material used in steel bars | 2φs15.2 | 2φs15.2 |
| Angle (°) | 18 | 18 |
| Borehole diameter (mm) | 150 | 150 |
| Total length (m) | 18 | 18 |
| Free segment length (m) | 12 | 12 |
| Anchorage length (m) | 6 | 6 |
| Prestress locking value (kN) | 90 | 90 |
| Design value of bearing capacity (kN) | 149.4 | 149.4 |

3.5.3. Design of Tensile Test Scheme

- (1) The anchor cable was stretched only after the slurry strength of the anchoring section became greater than 30 MPa and reached 80% of the designed strength grade;
- (2) Before tensioning, the anchor cables, jacks, anchoring tools, pressure plates and anchor hole center line were placed;
- (3) The technical Specification for Rock Bolt and Shotcrete Support Engineering (GB50086-2015) 12.1.21 requirements state the following: “Maximum load test: Permanent bolt

should take 1.2 times of the bolt tension design value, temporary bolt should take 1.1 times of the bolt tension design value". The acceptance test was loaded in stages, with the initial load being 10–20% of the designed load of the bolt and the graded load values being 0.4, 0.6, 0.8, 1.0 and 1.2 times of the designed load, respectively. The whole test was continuously loaded step by step. After the first load was stable, the next load could be applied until the maximum load was reached. The observation time for each stage was 10 min. Within the observation time for each stage, the cumulative displacement of the measuring anchor head displacement item was not intended to reach more than 1 mm before the next stage load was applied; otherwise, the observation time was extended. The final test load was also maintained for 10 min. If the displacement exceeded 1 mm within 10 min, the load was maintained for another 50 min the elongation was recorded at 15, 20, 25, 30, 45 and 60 min and the loading class and observation time for the anchor cable were recorded in the cable tensioning record table;

- (4) For the acceptance test, the design load, from 50% to the maximum test load, between the total displacement and the side was set to be greater than the load indicated by the theory for anchor bar free-segment lengths for prestressed elastic elongation (80%), and less than the free segment and 1/2 of the sum of the anchorage length indicated by prestressed reinforcement theory for elastic elongation and the anchor bar measured elongation and theory; the error was not greater than the theoretic elongation of plus or minus 6%;
- (5) Calculation of theoretical elongation: the formula for the theoretical elastic elongation in this acceptance test was calculated according to the provisions of article JT041-2004.12.8.3 of the technical Specification for Highway Bridge and Culvert Construction:

$$\Delta L = \frac{P_p L}{A_p E_p} \quad (4)$$

where P_p is the average tensile force of the prestressed reinforcement; L is the length of the prestressed reinforcement; the cross-sectional area of A_p is the prestressed reinforcement, which was here 141.4 mm²; and the elastic modulus of E_p is the prestressed reinforcement, which was here 193 GPa.

3.5.4. Test Process

The construction of the fast anchor cable included drilling, laying the anchor cable, grouting and tensioning. Holes were drilled into the construction unit according to the design requirements, and the diameter was 150 mm. Grouting with the "new type of high strength fast anchoring agent slurry" with a water-to-material ratio of 0.26~0.28 was adopted in the grouting construction. The bottom-grouting method was adopted and the bottom end of the catheter was inserted into the hole bottom (300~500 mm from the hole bottom is recommended). The grouting operation was continuous and compact had no interruptions during the process, so that the grouting work could be completed during the time when the initial injected slurry was still plastic. In the process of grouting, the pipe was withdrawn at a slow and uniform speed, and the grouting pipe was lifted while grouting. It is strictly prohibited to pull out the slurry level of the pipe in order to avoid the occurrence of pole-breaking accidents. The outlet of the pipe was always below the surface of the slurry in the hole to ensure that all the gas in the hole could escape. When there is slurry flowing out of the orifice, it means that the grouting is full and the operation should be stopped. The working pressure of the grouting pump met the design requirements, and the influence of pipeline losses on the grouting pressure during the grouting process were considered to ensure enough grouting pressure. The grouting was high-pressure grouting.

4. Results and Discussion

4.1. Mechanical Properties of the New Anchoring Agent

It can be seen from Figure 8 that the compressive strength of the new type of anchorage sample increased significantly with the increase in the water-to-material ratio and curing days. When the water-material ratio was 0.22 or 0.25, the compressive strength reached more than 30 MPa after curing for 1 day. Compared with the grouting material in traditional cement mortar, the time could be reduced by 80%.

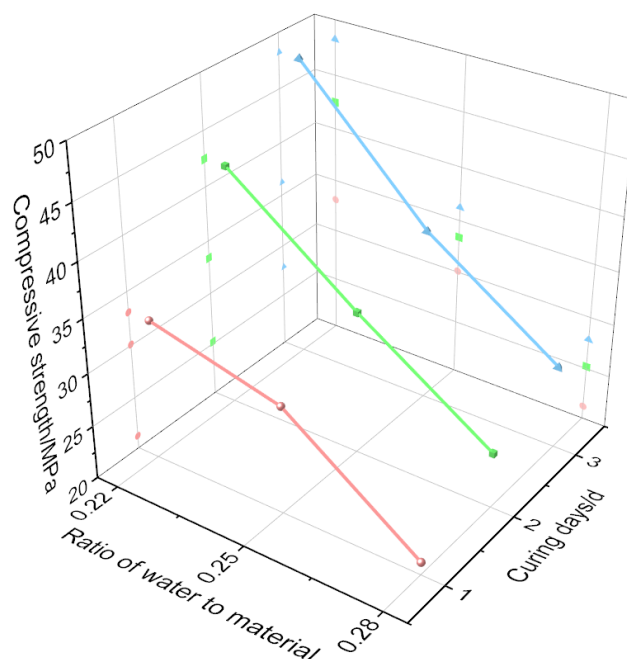


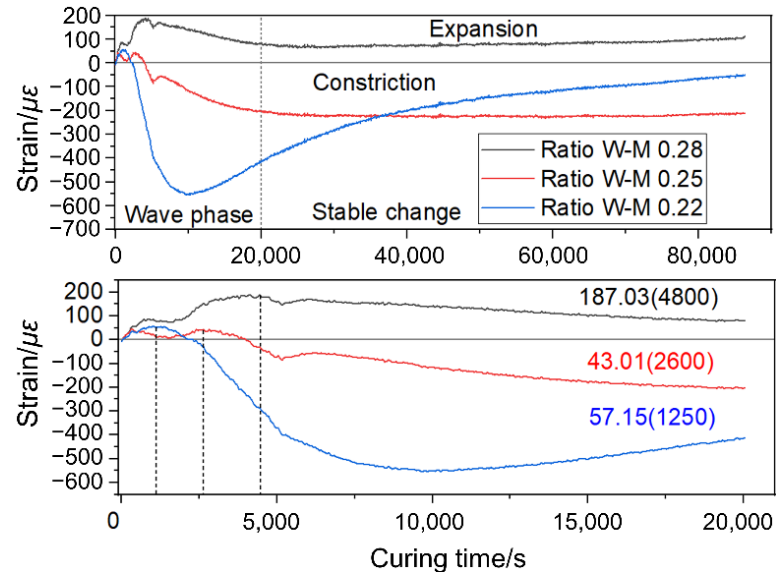
Figure 8. Compressive strength test results.

The compressive strength response to the water-material ratio was as follows: within the range of 0.22 to 0.25, the reduction rate for the compressive strength was 18.45%, and it was less than 25.77% within the range of 0.25 to 0.28, indicating that the water-material ratio had a greater influence on the compressive strength of the test block. The smaller the water-material ratio is, the more viscous the slurry is and the better its mechanical properties. The response of the compressive strength to the curing days was as follows: within 1 to 2 d, the rate of increase for the compressive strength was 19.41%, which was significantly higher than the rate of 10.70% obtained in 2 to 3 d, indicating that the compressive strength of the test block changed rapidly in the early stage and gradually slowed down after 3 days.

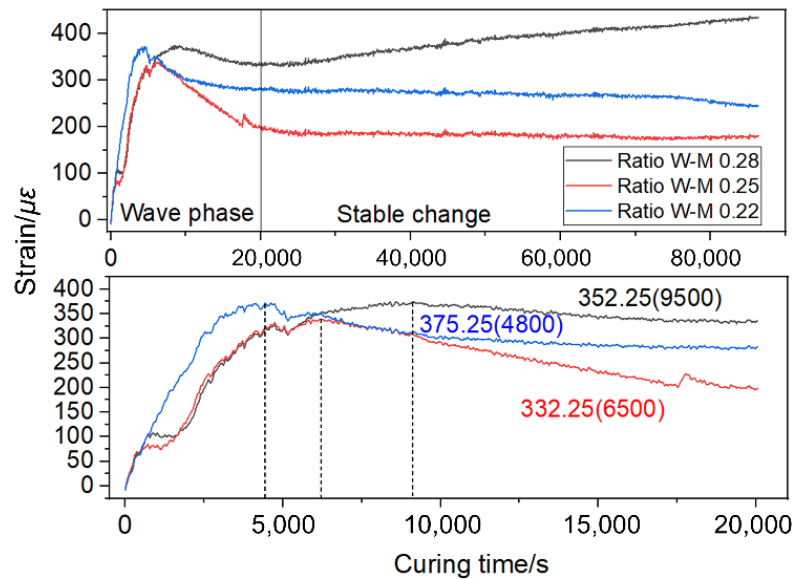
4.2. Characteristics of Free Solidification Strain

Figure 9 shows that the new free strain of the anchoring agent had an obvious stage, the stage of the cut-off point at 20,000 s, with this being the wave phase and showing the side-wall and bottom strain-growth cut rule. With the increase in the W-M ratio, the lateral expansibility of the anchor solid increased and a significant expansion and extrusion of the mold sidewalls occurred at a W-M ratio of 0.28; the strain gauges were stretched and the strain data became positive. At the same time, the peak strain showed obvious delays, suggesting that the more water components there were, the greater the liquidity, and greater the influence of gravity was, the greater the peak strain at the late time. At this stage, the anchoring agent and water reflected a major factor in the production of micro-expansibility, which was free strain. At this stage, the reaction between the anchoring agent and water was basically complete, but it still had a certain fluidity. The main control of its deformation was the self-gravity of the sample. Thus, it could be obtained that, under free conditions,

20,000 s (i.e., 5–6 h) was the critical point of the hydration reaction in the anchorage agent, and this was not significantly affected by the water–material ratio. Therefore, in practical applications, the environmental impact within 0–6 h after grouting should be addressed to avoid the formation of deformations as a result of the fluctuation in the anchorage strain. The strain gauge data were positive for tension and negative for compression.



(a) Lateral wall strain.



(b) Bottom strain

Figure 9. Free solidification strain under different water-to-material ratios.

4.3. Characteristics of Solidification Strain in Holes

It can be seen from Figure 10 that, under different water-to-material ratios, the anchor solid strain in the hole changed in accordance with the trend in curing days, showing a sharp increase first and then a steady increase. Moreover, the time node of the two stages was consistent with the hydration node of the free strain above roughly 5–6 h, and there was little feedback on the water-to-material ratio. Furthermore, with the increase in the water–material ratio, the peak hydration expansion in the grouting of the anchoring agent increased, and when the water–material ratio was small, the effect of the anchoring agent on reinforcement was greater than that on the wall of the borehole, while with the increase

in the water–material ratio, the effect of the anchoring agent on the bottom of the hole increased, indicating that the slurry with strong fluidity had strong expansibility at the bottom of hole. It can be seen that, when grouting in the borehole with broken rock at the bottom of the hole, in order to ensure the grouting effect, slurry with a slightly higher water-to-material ratio should be used for filling.

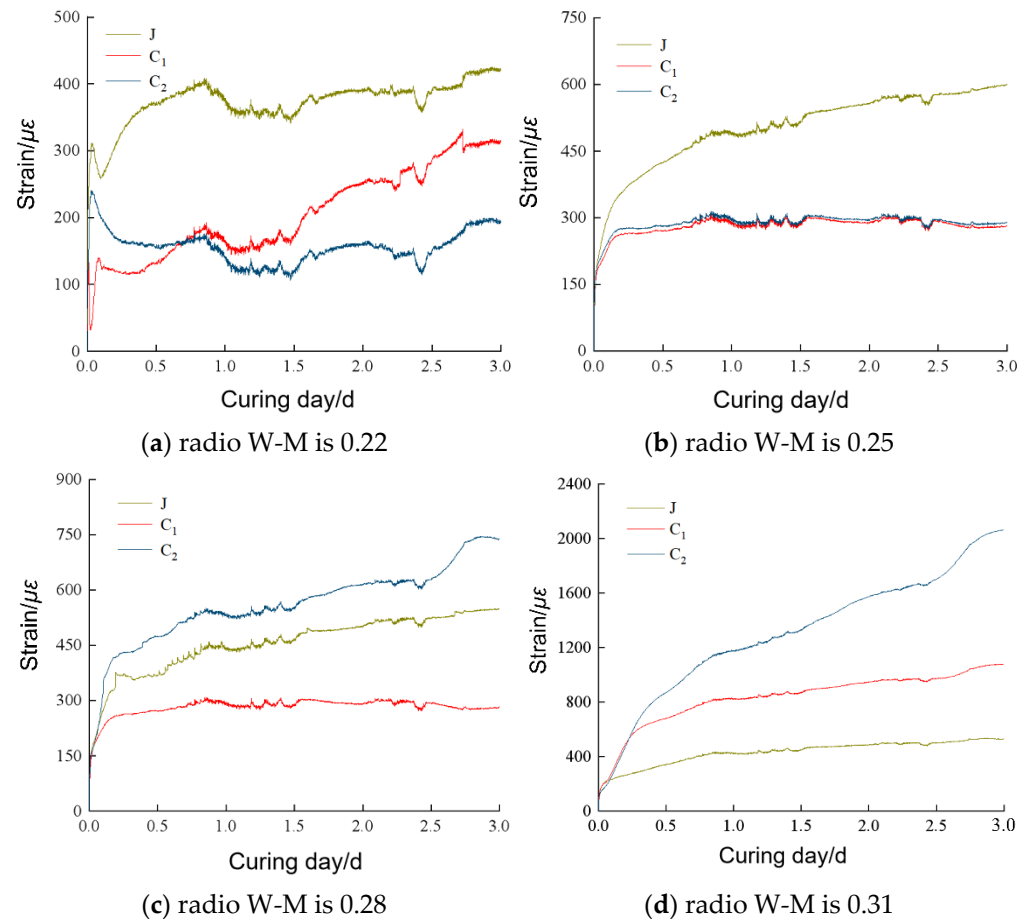


Figure 10. In-hole solidification strain at different water-to-material ratios.

4.4. Adhesion Characteristics

It can be seen from Figure 11 that, under different water and material conditions, the response of the strain at each position to pull-out differed to some extent. Under the condition of a water/material ratio of 0.22, the responses of the reinforcement and the hole wall to drawing force were synchronous. At 9.5 s and 6 kN, the reinforcement and hole wall showed reverse strains. At this time, the bonding force of the anchoring agent prevented the elongation of reinforcement and promoted the relative elongation of the hole wall until the drawing force reached 24.89 kN. Under the condition of a water/material ratio of 0.25, the responses of the steel reinforcement and hole wall to the drawing force were still synchronous. At 45 s and 10.1 kN, the steel reinforcement and hole wall showed reverse strains, and at 61.5 s and 13.2 kN, the steel reinforcement contraction reached the maximum value. After that, the reinforcement grouting became retractable, indicating that the steel reinforcement had been pulled out from the anchor solid. Similarly, under the conditions of water/material ratios of 0.28 and 0.31, the starting change trend was consistent with that when the water/material ratio was 0.25, and when the reinforcement was pulled out at 11 kN and 12 kN, respectively, the shrinkage of the reinforcement increased, indicating that its resistance to drawing was gradually becoming reduced.

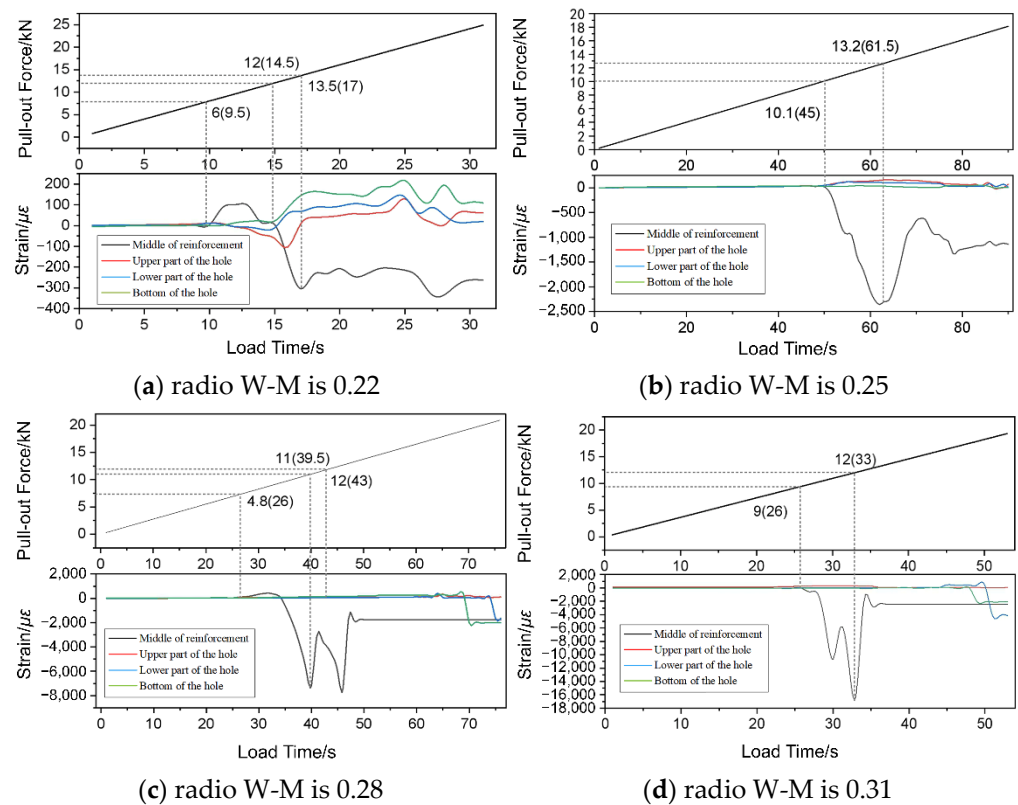


Figure 11. Drawing strain under different water–material ratio conditions.

To sum up, with the increase in the water–material ratio, the performance of the bonding of the new anchorage agent to the reinforcement gradually decreased. Therefore, in practical applications, through the control over the water–material ratio, increasing the contact area between the anchor cable and anchorage agent is an effective way to increase the anchorage performance.

4.5. On-Site Tensile Characteristics

Anchor cable tensioning was performed 30 h after the grouting of the test anchor cable. The obtained data are shown in Table 2.

Table 2. Summary of actual tension data.

| Tension Level | Tension (kN) | Hydraulic Gauge Reading (MPa) | Anchor Head Displacement Theory (mm) | Actual Anchor Head Displacement (mm) |
|-----------------|--------------|-------------------------------|--------------------------------------|--------------------------------------|
| Initial load | 27.7 | 2 | — | 9.3 |
| Level 1 loading | 57.3 | 4 | 14 | 19.3 |
| Level 2 loading | 86.8 | 6 | 28.9 | 28.2 |
| Level 3 loading | 116.4 | 8 | 38.8 | 37.6 |
| Level 4 loading | 145.9 | 10 | 48.6 | 48.2 |
| Level 5 loading | 175.4 | 12 | 58.4 | 56.6 |

According to the comparison and analysis of the data in Table 2, it can be concluded that the elongation was slightly larger or smaller than the increment of the theoretical value, which was ideal. In the five-stage loading process, the tensed-load reached 1.2 times the design load, and at this time, the displacement of the anchor cable increased steadily without an obvious failure of the anchor solid, indicating that the anchor solid exceeded the design strength and had good anchoring performance. Fast anchor cable construction technology

can meet the design requirements within 40 h. In the construction process, there were no obvious problems or environmental impact, in line with the construction requirements.

5. Conclusions and Prospects

We studied various aspects of the anchoring performance of a new, high-strength, fast anchorage agent by combining a laboratory test and field test and provided corresponding construction suggestions according to the performance. The conclusions are as follows:

- (1) The active SiO₂ content in the new, high-strength, fast anchorage agent was high and could react with Ca(OH)₂ to produce calcium silicate hydrate (2CaO·SiO₂·nH₂O), which was the main reason for its early strength;
- (2) According to the compressive strength test, the compressive strength of the new anchorage agent reached 30 MPa after 1 day, and its mechanical properties were highly sensitive to the water-to-material ratio. Therefore, the water-to-material ratio should be strictly controlled to ensure the agent's effectiveness;
- (3) According to the in-hole strain tests and the findings from free conditions, hydration reaction nodes with different water-to-material ratios acted for 5–6 h before the expansion performance reached its peak value;
- (4) The bonding of the anchoring agent to the rock layer was greater than the reinforcement, and the feedback of this property to the water–material ratio was not strong. Therefore, in actual construction, the contact area between the steel strand and the anchor solid should be increased to effectively increase the anchoring anchor cables;
- (5) Through an on-site anchor cable construction and drawing test, it was proved that the new anchoring agent could reach the designed drawing strength after 30 h, and its position value differed little from the calculation, indicating that the new, high-strength, fast anchoring agent could be effectively applied in field construction.

Author Contributions: Writing—original draft, H.L.; writing—review and editing, K.W.; validation, Z.D.; data curation and conceptualization, T.L. All authors have read and agreed to the published version of the manuscript.

Funding: This research was funded by the National Natural Science Foundation of China (U2006213), the National Natural Science Foundation of China (Science and Technology Activities Project) (42142041), and the Open Laboratory Fund (BHKF2021Z03).

Institutional Review Board Statement: Not applicable.

Informed Consent Statement: Not applicable.

Data Availability Statement: The data used to support the findings of this study are included within the article.

Conflicts of Interest: The authors declare no conflict of interest.

References

1. Ganesh, R. Vertical uplift resistance of close-spaced shallow rectangular group anchor plates embedded in sand. *Mar. Georesources Geotechnol.* **2020**, *38*, 1070–1081. [[CrossRef](#)]
2. Anamitra, R.; Paramita, B. Diameter effect on uplift capacity of horizontal circular anchor embedded in sand. *Int. J. Geotech. Eng.* **2020**, *14*, 779–792.
3. Guo, J. Recoverable resin bolt anchoring section anchoring characteristic study. *Coal Eng.* **2009**, *10*, 65–67.
4. Li, D. Application of fast hard cement coil bolt. *China Manganese Ind.* **1990**, *2*, 61.
5. Cui, P.; Dai, M.; Ding, Z. Research on anchorage bond performance of magnesium phosphate cement mortar and concrete. *China Build. Mater. Sci. Technol.* **2020**, *29*, 19–23.
6. Wang, Y.; Zhao, D.; Lu, W. Experimental research on destruction mode and anchoring performance of carbon fiber phyllostachys pubescens anchor rod with different forms. *Adv. Civ. Eng.* **2018**, *2018*, 1841267.
7. Xu, D.S.; Su, Z.Q.; Lalit, B.; Qin, Y. A hybrid FBG-based load and vibration transducer with a 3D fused deposition modelling approach. *Meas. Sci. Technol.* **2022**, *33*, 065106. [[CrossRef](#)]
8. Qin, Y.; Wang, Q.K.; Xu, D.S.; Yan, J.M.; Zhang, S.S. A FBG based earth and water pressure transducer with 3D fused deposition modeling approach for soil mass. *J. Rock Mech. Geotech. Eng.* **2022**, *14*, 663–669. [[CrossRef](#)]

9. Liu, S.; Wang, W.; Fu, M. Mechanical characteristics analysis and end shape optimization experiment of stirring anchoring agent for rebar bolts. *J. China Univ. Min. Technol.* **2020**, *49*, 419–427.
10. Bai, J.; Xue, X. Experimental study on loss of anchor cable pretension in situ. *Coal Sci. Technol.* **2020**, *41*, 50–51+63.
11. Yang, X.; Jia, S.; Wen, C. Development of a new inflatable controlled anchor system and experimental study of pull-out capacity. *Adv. Civ. Eng.* **2019**, *2019*, 8105986. [[CrossRef](#)]